Overcoming Coulomb Interaction Improves Free-Charge Generation and Thermoelectric Properties for n-Doped Conjugated Polymers

Liu, Jian; Shi, Yongqiang; Dong, Jingjin; Nugraha, Mohamad I.; Qiu, Xinkai; Su, Mengyao; Chiechi, Ryan C.; Baran, Derya; Portale, Giuseppe; Guo, Xugang

Published in:
ACS Energy Letters

DOI:
10.1021/acsenergylett.9b00977

Publication date:
2019

ACS Energy LETTERS

Cite This: ACS Energy Lett. 2019, 4, 1556−1564

http://pubs.acs.org/journal/aelccp

LETTER

Overcoming Coulomb Interaction Improves Free-Charge Generation and Thermoelectric Properties for n-Doped Conjugated Polymers

Jian Liu,*[,†] Yongqiang Shi,[‡] Jingjin Dong,[†] Mohamad I. Nugraha,[§] Xinkai Qiu,[†,∥] Mengyao Su,[‡] Ryan C. Chiechi,[†,∥] Derya Baran,[§] Giuseppe Portale,[†] Xugang Guo,*[,‡] and L. Jan Anton Koster*[,†]

[†]Zernike Institute for Advanced Materials, University of Groningen, Nijenborgh 4, 9747 AGGroningen, The Netherlands

[‡]Department of Materials Science and Engineering and The Shenzhen Key Laboratory for Printed Organic Electronics, Southern University of Science and Technology (SUSTech) No. 1088, Xueyuan Road, Shenzhen, Guangdong 518055, China

[§]King Abdullah University of Science and Technology (KAUST), Physical Sciences and Engineering Division (PSE), KAUST Solar Center (KSC), Thuwal 23955-6900, Saudi Arabia

[∥]Stratingh Institute for Chemistry, University of Groningen, Nijenborgh 4, 9747 AG Groningen, The Netherlands

Supporting Information

ABSTRACT: **Molecular doping of organic semiconductors creates Coulombically bound charge and counterion pairs through a charge-transfer process. However, their Coulomb interactions and strategies to mitigate their effects have been rarely addressed. Here, we report that the number of free charges and thermoelectric properties are greatly enhanced by overcoming the Coulomb interaction in an n-doped conjugated polymer. Poly(2,2′-bithiazolothienyl-4,4′,10,10′-tetracarboxydiimide) (PDTzTI) and the benchmark N2200 are n-doped by tetrakis (dimethylamino) ethylene (TDAE) for thermoelectrics. Doped PDTzTI exhibits ∼10 times higher free-charge density and 500 times higher conductivity than doped N2200, leading to a power factor of 7.6 μW m^{-1} K^{-2} and ZT of 0.01 at room temperature. Compared to N2200, PDTzTI features a better molecular ordering and two-dimensional charge delocalization, which help overcome the Coulomb interaction in the doped state. Consequently, free charges are more easily generated from charge−counterion pairs. This work provides a strategy for improving n-type thermoelectrics by tackling electrostatic interactions.**

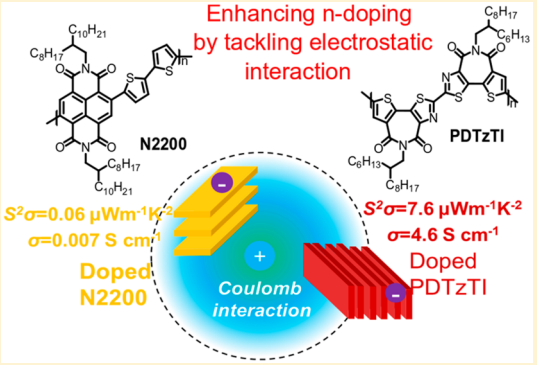

Molecular doping is an effective strategy for modifying the electronic properties of conjugated polymers for a variety of organic optoelectronic devices.[1−4] For emerging organic thermoelectrics (OTEs), doping is used to modulate carrier density (n), thereby optimizing thermoelectric properties [i.e., electrical conductivity (σ), Seebeck coefficient (S), and power factor ($S^2\sigma$)].[5−10] Doping of the organic materials normally occurs in two steps.[11] First, integer or partial charge transfer (CT) between host and dopant molecules occurs, forming Coulombically bounded charge and counterion pairs, hereafter referred to as a charge-transfer complex (CTC).[12−14] It is worth mentioning that such a CTC is not specific for the integer or partial CT. In the secondary step, the CTC creates free charges through thermal ionization. Typically, conjugated polymers have low dielectric constants ($\varepsilon_r \approx 3$),[15] which are expected to lead to binding energies of the CTC on the order of several hundred millielectronvolts.[14,16] Such strong Coulomb interaction reduces the number of free charges and subsequently the doping efficiency.[14] Moreover, as noted by several theoretical studies, the counterions are likely to broaden the density of states (DOS) and act as Coulomb traps to reduce the carrier mobility.[17,18] Nevertheless, the critical question of how to overcome the Coulomb interaction has been rarely addressed in organic thermoelectrics. More importantly, there has been a lack of deep understanding how the molecular structure influences the doping process and thermoelectric properties.

Poly{[N,N'-bis(2-octyldodecyl)-naphthalene-1,4,5,8-bis-(dicarboximide)-2,6-diyl] (NDI)-*alt*-5,5′-(2,2′-bithiophene)

Received: May 6, 2019
Accepted: June 10, 2019
Published: June 10, 2019

DOI: 10.1021/acsenergylett.9b00977
ACS Energy Lett. 2019, 4, 1556−1564

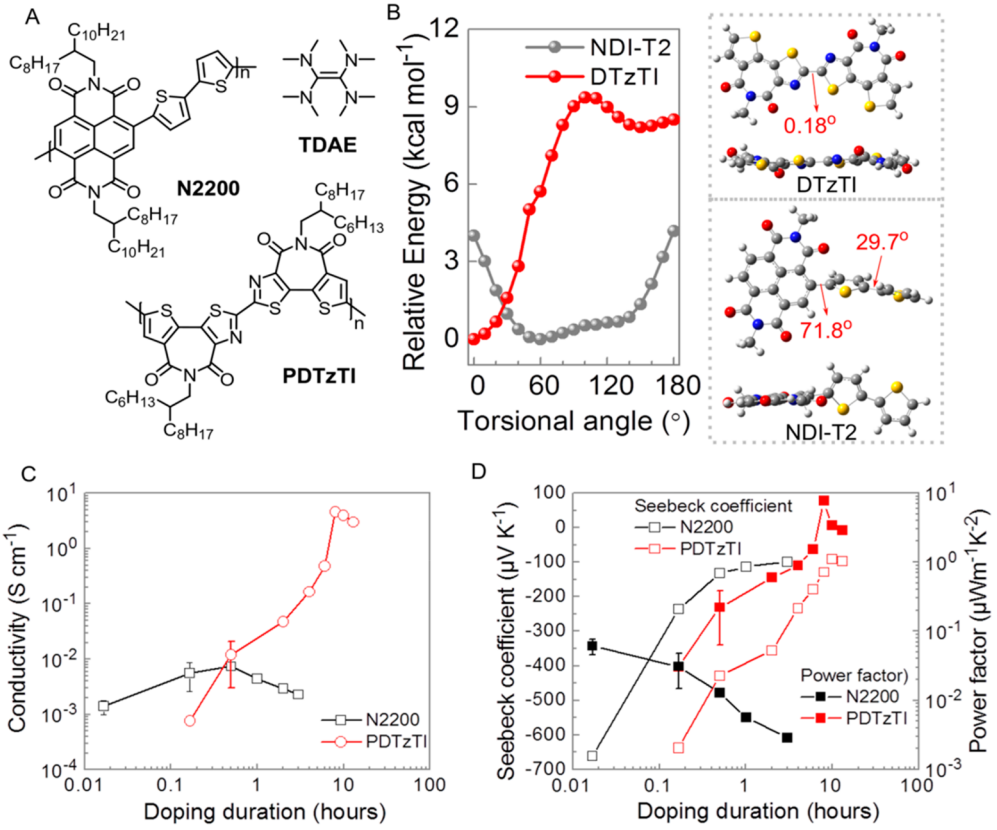

Figure 1. (A) Molecular structures of hosts (N2200 and PDTzTI) and dopant TDAE. (B) ωB97XD/6-31G(d, p) relaxed potential energy as a function of torsional angle for the repeating unit NDI-T2 and DTzTI of polymer semiconductor N2200 and PDTzTI, respectively. The side chains were truncated to methyl for calculation simplicity. (C) Electrical conductivity and (D) Seebeck coefficient and power factor values of N2200 and PDTzTI films exposed to TDAE vapor for different periods.

(T2)} (N2200) is a benchmark n-type donor−acceptor (D−A) conjugated polymer with a large electron affinity and good electron mobility (μ_e) of >0.1 $cm^2\ V^{-1}\ s^{-1}$ in organic thin-film transistors (OTFTs).[19−21] As the first trial for n-type polymeric thermoelectrics, n-doping of N2200, however, yields a low electrical conductivity of ~1×10^{-3} S cm^{-1} and power factor of 0.1 μW m^{-1} K^{-2}.[22] Afterward, numerous research efforts have been stimulated to design better n-type conjugated polymers for OTEs by modifying the backbones and side chains to achieve favorable energetics, high electron mobility, planar structure, and good host/dopant miscibility.[23−33] For example, Wang et al. reported increased backbone planarity, π-stacking, and electron affinity in an NDI-based D−A copolymer by using bithiazole rather than bithiophene as donor moiety.[33] Pei and co-workers reported enhanced thermoelectric performance by tuning electron affinity and improving electron mobility through the use of halogen-atom substituted backbone.[23,26] Recently, we demonstrated that by embedding sp^2-N into the donor moiety, the DOS distributions of the D−A copolymer can be tailored.[24] By doing so, the electrical conductivity is improved by a factor of >1000. Particularly, the use of polar glycol ether side chains has been reported by us and other groups to effectively increase the host/dopant miscibility and thus improve the doping efficiency of n-doped conjugated polymers.[27−29] Most of the previous works improve the n-doping of conjugated polymers by tuning factors influencing the first step of the doping process. Despite fast progress, the fundamental question regarding which properties of the host or dopant materials govern the electrostatics in a doped film has been open for inquiry thus far. Recently, we demonstrated that in lightly n-doped fullerene derivatives, the polar glycol ether side chains help screen the Coulomb interaction and boost the doping efficiency to values approaching 100%.[34] Schwartz and co-workers proposed that shielding charges (polarons) from counterions by a steric cluster dopant dramatically increases the number of free charges and carrier mobility in a p-doped conjugated polymer.[35] However, there has been no report addressing how to effectively overcome the Coulomb interaction in an n-doped conjugated polymer for advancing n-type organic thermoelectrics.

Here, we report that the number of free charges and thermoelectric properties can be dramatically enhanced by overcoming the Coulomb interaction in an n-doped conjugated polymer. Poly(2,2′-bithiazolothienyl-4,4′,10,10′-tetracarboxydiimide) (PDTzTI), a recently developed acceptor−acceptor (A−A) homopolymer with good n-type transport behavior in organic field-effect transistors,[36] has not been investigated in thermoelectric devices. We selected PDTzTI and the benchmark N2200 as the host for n-type thermoelectrics. Under the optimized doping conditions, PDTzTI shows ~10 times higher free-charge density and 500 times higher conductivity compared to those of N2200. Hence, the doped PDTzTI displays a remarkable power factor of 7.6 μW m^{-1} K^{-2} and figure of merit ZT of 0.01, which represents one of the best results for n-type polymeric thermoelectrics. Such dramatic performance enhancement in doped PDTzTI is mainly attributed to the mitigated Coulomb interaction

DOI: 10.1021/acsenergylett.9b00977
ACS Energy Lett. 2019, 4, 1556−1564

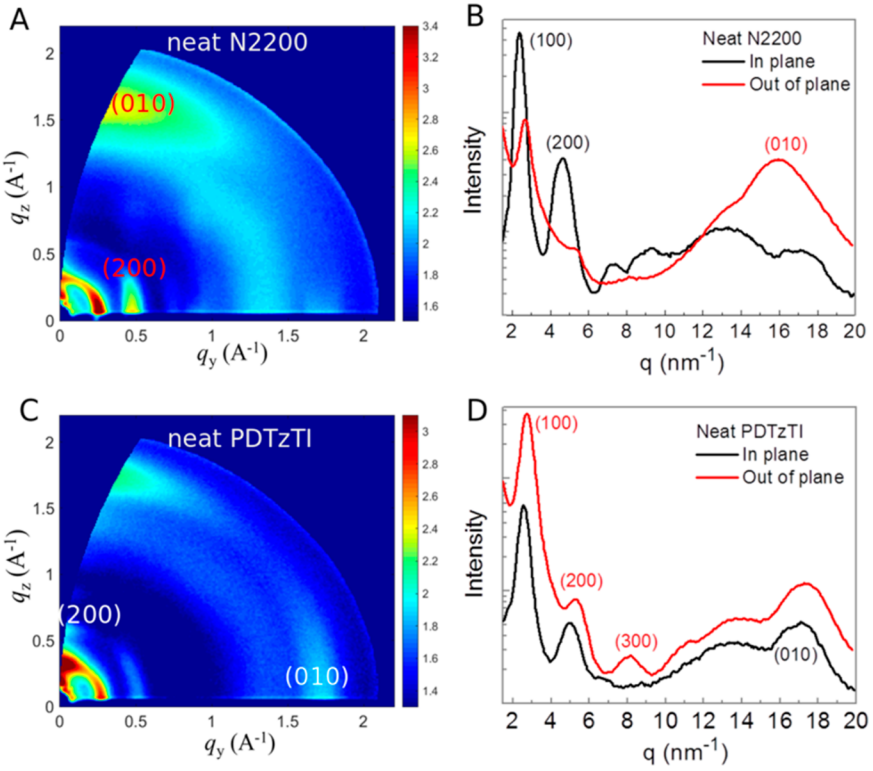

Figure 2. Molecular packing in neat thin films. 2D GIWAXS patterns (A and C) and linecuts in the in-plane and out-of-plane directions (B and D) for neat N2200 and PDTzTI films, respectively.

compared to that of N2200. In particular, PDTzTI chains pack into larger crystal domains, which keep the counterions far from the charges on polymer chains, therefore increasing the chance of charges escaping from the counterions. Moreover, enhanced molecular planarity and packing density of PDTzTI together with minimized D−A character promote two-dimensional charge delocalization, which helps charges escape from the Coulomb interaction. As such, the CTCs are more easily dissociated into free charges in doped PDTzTI. Our study provides insight into the doping process of conjugated polymers and could be helpful for future material design for advancing n-type organic thermoelectrics.

Figure 1A displays the chemical structures of the host conjugated polymers (PDTzTI versus N2200) and an n-type dopant, tetrakis (dimethylamino) ethylene (TDAE). In spite of the electron-rich character of thiophene or thiazole in the backbone, the highly electron-withdrawing imide group strengthens the building block DTzTI as an electron acceptor.[36−39] Consequently, PDTzTI is a typical A−A homopolymer (versus the D−A copolymer N2200).[36] In comparison to thiophene, thiazole in the building block can reduce the steric hindrance and promote intramoleclar noncovalent N···S interactions.[40] These aspects are expected to increase the backbone planarity. Indeed, based on density functional theory (DFT) calculations in Figure 1B, the DTzTI backbone displays a completely planar conformation with a very small energy-minimized dihedral angle of 0.18°, as compared to that (72°) of the N2200 repeat unit. The improved backbone planarity is intended to facilitate a better packing order and charge delocalization for PDTzTI.[33]

The cyclic voltammetry characterization of N2200 and PDTzTI thin films was performed to study the effects of backbone structure on the energetics (Figure S1). PDTzTI and N2200 show an identical lowest unoccupied molecular orbital (LUMO) level of −3.8 eV. The similar LUMOs indicate the high electron affinities of the two conjugated polymers, enabled by the strong electron-withdrawing imide groups. Notably, the influences of the energetics on the doping process could be excluded in the present study. TDAE vapor-soaking proves to be an effective n-doping method for many conjugated polymers with alkyl side chains including N2200.[32,33] Moreover, doping occurs after film formation, which has been recently pointed out to have minimized effects on the morphology of the active layer.[41] Hence, this method was employed to dope n-type conjugated polymers in this work as well (see the Supporting Information for details).

Figure 1C shows the four-point electrical conductivities of N2200 and PDTzTI films soaked in the TDAE vapor for varying periods (Figure S2). The neat N2200 and PDTzTI films show very low electrical conductivities of 1.0×10^{-10} S cm^{-1} and 9×10^{-10} S cm^{-1}, respectively. Doping N2200 quickly results in a peak electrical conductivity of 7×10^{-3} S cm^{-1} after TDAE soaking for 30 min. In contrast, it takes 8 h of doping for PDTzTI to reach its optimized electrical conductivity of 4.6 S cm^{-1}, which represents one of the best conductivities for n-doped conjugated polymers (Table S1).

Figure 1D displays the Seebeck coefficients and power factors of doped N2200 and PDTzTI films (Figure S3). The Seebeck coefficient of the doped N2200 film was changed from −662 to −99.7 μV K^{-1} by modulating the soaking time from 1 min to 3 h. The negative sign of the Seebeck coefficient differentiates electrons as the dominant charge carriers. The PDTzTI film exposed to TDAE vapor for 10 min exhibits a Seebeck coefficient of −638 μV K^{-1}. When the soaking time is increased up to 8 h, the Seebeck coefficient of doped PDTzTI gradually decreases to −129 μV K^{-1}. The Seebeck coefficient is

DOI: 10.1021/acsenergylett.9b00977
ACS Energy Lett. 2019, 4, 1556−1564

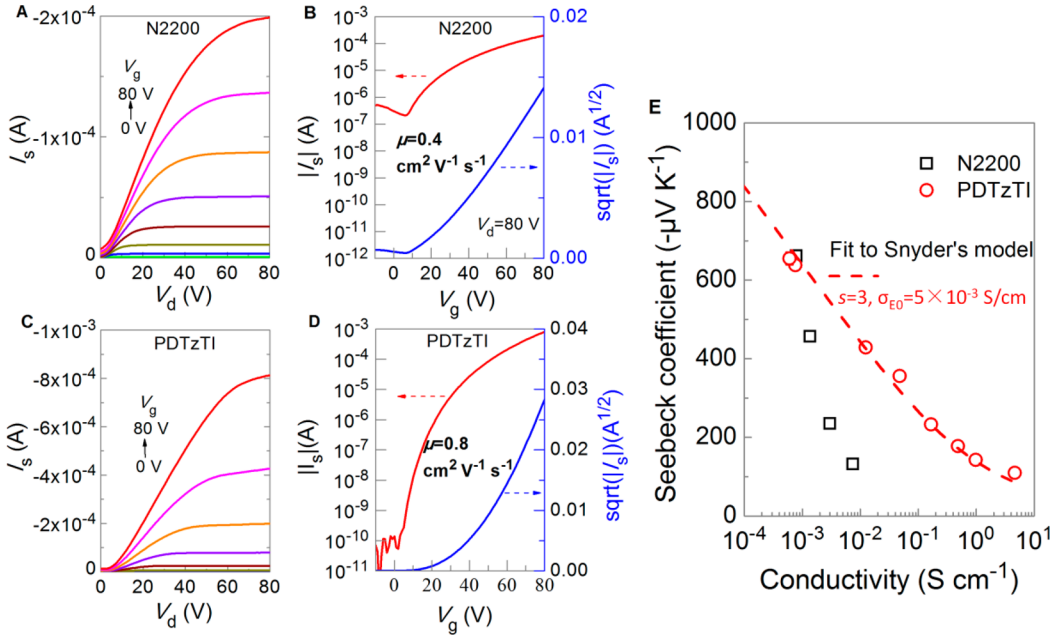

Figure 3. Top-gate/bottom-contact OTFT output and transfer characteristics of (A and B) N2200- and (C and D) PDTzTI-based devices. (E) Plots of $S-\sigma$ relations for doped N2200 and doped PDTzTI films and the fit to Snyder's model (s = 3 and σ_{E0} = 5 × 10^{-3} S cm^{-1}).

determined by the difference between the Fermi energy level (E_F) and the transport energy level (E_T).[32] The reduced absolute Seebeck coefficients indicate increased doping levels with the E_F moving toward the E_T.[42] At a soaking time of 8 h, an optimized power factor of 7.6 μW m^{-1} K^{-2} was achieved in doped PDTzTI, which is much higher than that (0.06 μW m^{-1} K^{-2}) of doped N2200 films. This represents one of the best results for n-type polymeric thermoelectrics (Table S1). We measured the in-plane thermal conductivity ($\kappa_{\parallel}$) of PDTzTI film before and after the doping process (see details in the Supporting Information). It was found that the doping process exerts a negligible influence on $\kappa_{\parallel}$, and the doped PDTzTI at a soaking time of 8 h exhibits a $\kappa_{\parallel}$ of 0.22 ± 0.02 W m^{-1} K^{-1} at room temperature (Table S2). The figure of merit ZT for doped PDTzTI was accordingly calculated to be 0.01 at room temperature.

The two-dimensional (2D) grazing incidence wide-angle X-ray scattering (GIWAXS) patterns and corresponding linecuts of the neat N2200 and PDTzTI films are displayed in Figure 2. Both polymers adopt a mixed face-on and edge-on orientation. The N2200 chain tends to pack mostly with a face-on orientation relative to the substrate, while the PDTzTI chain prefers the edge-on orientation. For neat N2200, the (100) and (200) peaks at 0.25 and 0.51 Å^{-1} along the out-of-plane direction were clearly seen. For neat PDTzTI film, the (100), (200), and (300) peaks at q_z = 0.27, 0.54, and 0.81 Å^{-1} were observed, respectively. The two polymers exhibit a (010) reflection at q_z = 1.6 Å^{-1} for N2200 and q_{xy} = 1.72 Å^{-1} for PDTzTI, associated with $\pi-\pi$ stacking distances of ~3.9 and ~3.6 Å, respectively. The smaller spacing for PDTzTI indicates a much closer π-stacking, which is likely a consequence of having a more planar backbone. Additionally, the π-stacking coherence length of PDTzTI is 26 Å, which is larger than that (19 Å) of N2200; the same holds true for the lamellar coherence length (150 Å versus 98 Å). As such, PDTzTI has a higher crystallinity than N2200. The doping process exerts slight influences on the extent of the developed crystallinity and the chain packing orientation (Figure S5). Figure S6 displays the surface morphologies of neat films and doped films for different periods measured by atomic force microscopy (AFM). Both neat N2200 and PDTzTI films show fibril-textured morphologies, which are expected to facilitate the charge transport. The TDAE vapor doping of these polymers appears not to influence their morphologies. These results indicate that vapor doping has minimized effects on the crystalline microstructures, which constitute the primary charge transport network.

To compare the charge transport between N2200 and PDTzTI films in the undoped state, we fabricated top-gate/bottom-contact (TGBC) OTFTs with a device structure of glass/Au/neat n-type polymer/CYTOP/Al. Panels A–D of Figure 3 display the corresponding output and transfer characteristics of the OTFTs. The devices based on N2200 and PDTzTI have comparable and high average saturation electron mobilities of 0.4 and 0.8 cm^2 V^{-1} s^{-1}, respectively. The large difference in electrical conductivity between the doped N2200 and PDTzTI is, therefore, unlikely to originate from their intrinsic charge transport properties but is specific to the doped state. To gain an insight into the mechanism by which charges move in the doped states, we investigated the $S-\sigma$ relationships (Figure 3E). We then attempted to fit the $S-\sigma$ curve of doped PDTzTI by using Snyder's model,[43] which has been reported to properly portray the evolution of thermoelectric parameters with varying doping levels for many doped organic systems.[27,43,45] The derived characteristic shape of the $S-\sigma$ curve was recently rationalized by Kemerink et al. in a classical Mott-type variable-range hopping model.[44] The best fit in a broad range of conductivity for doped PDTzTI was obtained with a transport parameter of s = 3 and transport coefficient of σ_{E0} = 5 × 10^{-3} S cm^{-1}. It is interesting to note that the $S-\sigma$ of doped N2200 follows the same fit at a soaking time of 1 min. It suggests that the charge transport in doped N2200 behaves similarly to that in doped PDTzTI at very low doping, which is to be expected given the similar OTFT mobilities and energetics of both polymers. However, further doping of N2200 leads to a faster change in S with σ

DOI: 10.1021/acsenergylett.9b00977
ACS Energy Lett. 2019, 4, 1556–1564

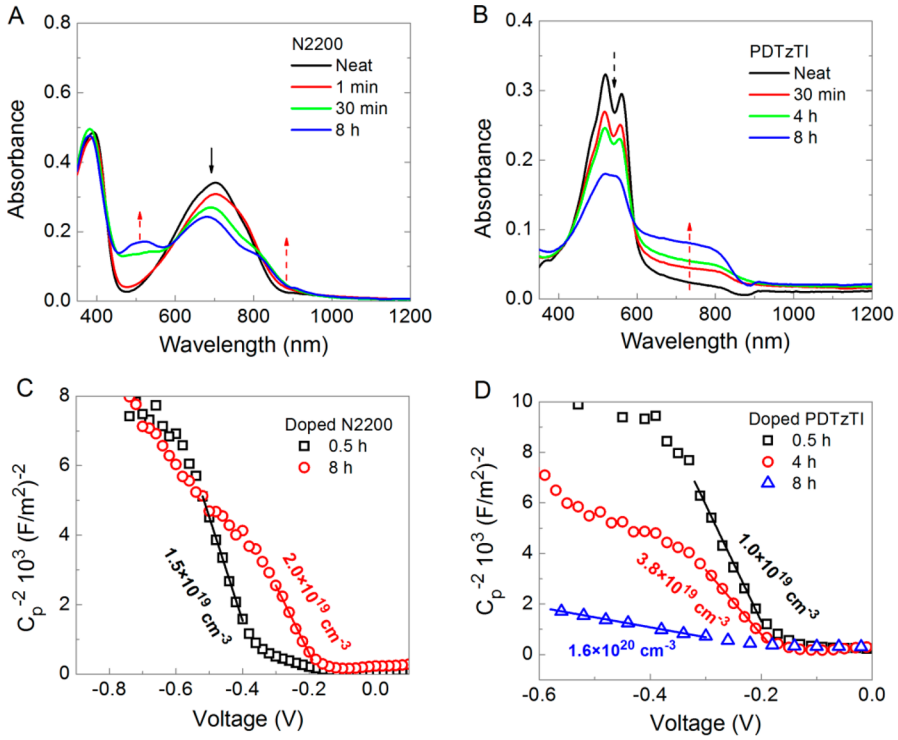

Figure 4. UV−vis−NIR absorption spectra of the neat and doped films of (A) N2200 and (B) PDTzTI and Mott−Schottky plots of (C) TDAE-doped N2200 and (D) TDAE-doped PDTzTI films for different periods. The capacitances were measured at a frequency of 10 Hz, and the extracted free-charge densities are indicated next to the corresponding curves.

than that of doped PDTzTI. Fitting the $S-\sigma$ curve of doped N2200 with Snyder's model is impossible, and we surmise that σ_{E0} is not contstant with varying doping level.

Incorporating dopant molecules into the host matrix may disrupt the microstructure of the latter, leading to degradated charge transport. This possibility can be almost excluded here because of the minimized effects of vapor doping on the microstructure (as evidenced by GIWAXS and AFM results). Alternatively, the doping process generates charges and counterions. The latter is able to adversely impact charge transport in a variety of pathways, such as broadening the DOS and inducing deep Coulomb traps.[17,18,44] It appears that the charge transport of doped PDTzTI was more tolerant to the presence of counterions, showing a consistent charge transport mechanism at a wide range of doping levels. In contrast, by furthering the doping level of N2200, the number of counterions increases and free charges are more easily captured by the Coulomb traps, causing degraded charge transport with decreasing σ_{E0}. Why PDTzTI is more tolerant to counterions than N2200 and the evidence of the Coulomb traps in the latter system will be discussed in later sections.

Panels A and B of Figure 4 show the UV−vis−NIR absorption spectra of neat and doped N2200 and PDTzTI films. The neat N2200 thin film exhibits two characteristic neutral peaks at 390 and 706 nm, which are assigned to the $\pi-\pi^*$ transition and an intramolecular charge-transfer transition, respectively.[46] However, the neat PDTzTI film displays two higher-energy adjacent neutral peaks at 519 and 560 nm. Upon TDAE doping, the transitions in those neutral spectral peaks gradually decrease in intensity, accompanied by the appearance of two absorption bands located at approximately 500 and 820 nm for N2200. These new spectral features are attributed to the polaron-induced transitions.[27,32,47] We speculate that doping PDTzTI induces such polaron transition as well, leading to a new absorption band between 620 and 900 nm.

As explicated in the introduction, the molecular doping is a two-step process. Generally, the loss of the transitions in the original spectra of the neat polymer films is caused by the first step, that is, the formation of CTC.[14] At a soaking of 30 min, the original peak intensity of N2200 decreased by 27%, while that of PDTzTI decreased by 20%. After 8 h, the original peak intensities of N2200 and PDTzTI decreased by 30% and 34%, respectively. These results indicate that more time is required for TDAE vapor to dope the PDTzTI film than the N2200, possibly because the former is more closely packed with a higher crystallinity and an edge-on dominated orientation (see GIWAXS data in Figure 2). Eventually the extent to which the host molecules react with the dopant to form CTCs is comparable between N2200 and PDTzTI. However, the similar extent of this reaction does not necessarily translate into a similar number of free-charge carriers, as charges in CTCs need to overcome the Coulomb interaction to actually become "free".

We measured the free-carrier density (n) by using admittance spectroscopy on ion-gel-based metal−insulator−semiconductor (MIS) devices (see details in the Supporting Information).[27] Panels C and D of Figure 4 display the Mott−Schottky plots of MIS devices based on doped N2200 and PDTzTI films. The Mott−Schottky analysis gives free-carrier density as[48]

$$n = \frac{2}{q\varepsilon_0\varepsilon_r \frac{\partial C_p^{-2}}{\partial V}} \quad (1)$$

DOI: 10.1021/acsenergylett.9b00977
ACS Energy Lett. 2019, 4, 1556−1564

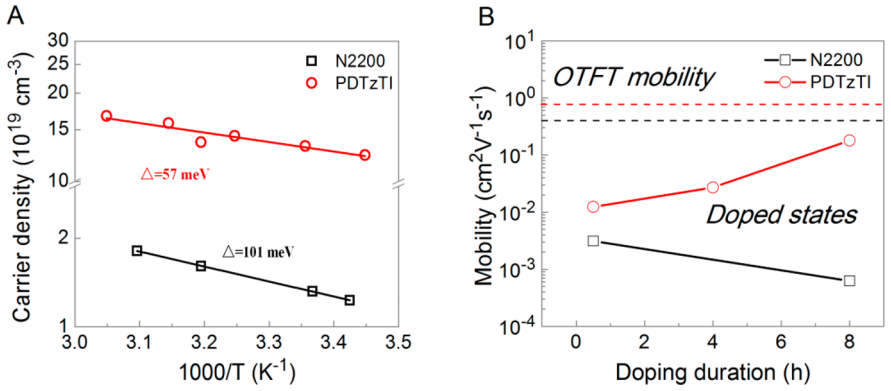

Figure 5. Temperature-dependent (A) carrier density in the doped N2200 and PDTzTI and (B) the bulk mobilities in various doped polymer films. (The black and red horizontal dashed lines represent OTFT mobilities of neat N2200 and PDTzTI films, respectively.)

Table 1. Summarized Material Parameters of Neat and Doped N2200 and PDTzTI Thin Films

host	LUMO[a] (eV)	OTFT μ (cm^2 V^{-1} s^{-1})	σ_{max} (S cm^{-1})	$S^2\sigma$ (μW m^{-1} K^{-2})	ZT	n^b ($\times 10^{19}$ cm^{-3})	bulk μ^b (cm^2 V^{-1} s^{-1})
N2200	−3.8	0.4	0.007	0.06		1.5 ± 0.3	0.003
PDTzTI	−3.8	0.8	4.6	7.6 ± 0.5	0.01	16 ± 6	0.2

[a] $E_{LUMO} = -e(E_{red}^{onset} + 4.8)$ eV,[36] where E_{red}^{onset} is the onset reduction potential versus Fc/Fc$^+$ in the cyclic voltammetry curve. [b] Free-charge density extracted from Mott−Schottky analysis at the point of maximum electrical conductivity.

where ε_r and C_p are the dielectric constant of the active layer and the total capacitance of the MIS devices, respectively. The doped N2200 soaked in TDAE vapor for 0.5 h exhibits a free-carrier density of $(1.5 \pm 0.3) \times 10^{19}$ cm^{-3}, which slightly increases to $(2.1 \pm 0.3) \times 10^{19}$ cm^{-3} after 8 h of soaking. The doped PDTzTI film shows a free-carrier density of 1.0×10^{19} cm^{-3} at a soaking time of 0.5 h. After 4 and 8 h of soaking, the free-carrier density increases to $(3.8 \pm 1.2) \times 10^{19}$ and $(1.6 \pm 0.6) \times 10^{20}$ cm^{-3}, respectively. Assuming the total site density of 8×10^{20} cm^{-3},[49] the doping levels of the doped N2200 and PDTzTI films at a soaking time of 8 h were determined to be 0.026 and 0.2, respectively. Apparently, PDTzTI was doped with many more free charges generated than N2200.

Why are the CTCs in the doped PDTzTI system more easily dissociated to yield free charges than those in the case of N2200? This question pushed us toward exploring factors which could impact the Coulomb interaction. On the one hand, the extremely planar PDTzTI chains tend to π-stack into larger crystalline domains than those of N2200, which was evidenced by GIWAXS data (Figure 2). A large crystalline domain could potentially keep the counterion distant from the charge residing on the polymer, therefore increasing the chance of charges escaping from the Coulomb interaction. On the other hand, the answer might be best framed in terms of charge generation in organic photovoltaics (OPV). In a donor/acceptor blend organic photovoltaic device, the photoinduced charge-transfer (CT) process gives rise to bound electron−hole pairs (CT states) at heterojunction interfaces, and sequential charge generation requires a driving energy to overcome the Coulomb interaction existing in the CT states.[50,51] It is well-established that charge delocalization can promote the dissociation of CT states into long-range separated charge carriers.[52] We hypothesized that free-charge generation from CTCs in doped organic systems may be analogous to charge generation in OPV devices. As N2200 is a typical donor−acceptor type copolymer, charges (polarons) are largely localized within a few repeating units because of backbone distortion or asymmetric relaxations of the two moieties after charging.[53,54] In stark contrast, PDTzTI is an acceptor−acceptor type homopolymer with a completely planar backbone, allowing for a homogeneous relaxation along the intrachain direction in a charged state. Additionally, the large polarity of thiazole core enhances the intermolecular interaction for tight packing, enabling a spatially extended π-system. Earlier studies on regioregular poly-3-hexylthiophene showed, by means of optical spectroscopy, that interchain order or coupling plays a decisive role in the formation of delocalization polarons.[55,56] In a similar sense, the molecular motif of PDTzTI promotes a better charge delocalization over intra- and intermolecular directions. As such, the improved charge delocalization in doped PDTzTI might also contribute to facilitate the CTC dissociation into free charges compared to doped N2200.

Therefore, we suggest that the higher yield of free charges from CTCs in doped PDTzTI may stem from the mitigated Coulomb interaction governed by its crystalline properties together with an improved two-dimensional charge delocalization. The free charges are generated from the CTCs by the following equation:[14]

$$n \approx N_{CTC}^{+} = \frac{N_{CTC}}{1 + \exp[(E_F - E_{CTC})/(k_B T)]} \quad (2)$$

where N_{CTC}^{+}, N_{CTC}, and E_{CTC} are the density of ionized CTC states, the total density of CTCs, and the energy of CTCs, respectively. Easier free-charge generation in doped PDTzTI should correspond to a smaller activation energy (Δ) of free charge. To verify this point, we performed Mott−Schottky analysis on the doped N2200 and PDTzTI films under temperature variations (Figure S7). Figure 5A shows the Arrhenius-type plots of the carrier density versus temperature. The extracted activation energy Δ in the doped N2200 film is 101 meV. Indeed, the doped PDTzTI exhibits a much smaller Δ of 57 meV. A recent study conducted by Tietze et al. suggested that a large energetic disorder could lead to a small Δ.[14] This possibility can be almost excluded here, as PDTzTI shows a high molecular order (see the GIWAXS and AFM

DOI: 10.1021/acsenergylett.9b00977
ACS Energy Lett. 2019, 4, 1556−1564

data), high OTFT mobility of 0.8 $cm^2\ V^{-1}\ s^{-1}$, and near temperature independence of Seebeck coefficient (Figure S8A).[33] Therefore, a lower activation energy Δ results from easier dissociation of CTCs and hence corresponds to an increased number of free charges at a given density of CTCs.

In the following we continue to explore the effects of the Coulomb interaction on the charge transport in the two doped films. The bulk mobilities of doped films were calculated on the basis of the formula $\sigma = \mu \times n \times q$ and are displayed together with the OTFT mobilities in Figure 5B and Table 1. Regardless of their similar OTFT mobilities, the two molecularly doped conjugated polymers exhibit very distinct bulk mobilities. At the point of maximum conductivity, the doped PDTzTI presents a bulk mobility of 0.2 $cm^2\ V^{-1}\ s^{-1}$, much higher than that ($3 \times 10^{-3}\ cm^2\ V^{-1}\ s^{-1}$) of the doped N2200. The lower bulk mobility of the doped N2200 further proves the adverse effects caused by the counterions. In contrast, the doped PDTzTI displays a mobility similar to that derived from "'counterion-free"' OTFT devices. It therefore strongly indicates a greatly mitigated Coulomb interaction in doped PDTzTI.

The Arrhenius-type plots of the electrical conductivity for the doped N2200 and PDTzTI films are displayed in Figure S8B. The extracted activation energies (E_{ac}) for doped N2200 and PDTzTI are 222 and 71 meV, respectively. E_{ac} is the sum of the activation energies of the mobility and the carrier density. Hence, the activation energy of mobility was calculated to be 121 meV for the doped N2200 and 14 meV for the doped PDTzTI. In a disordered system, charge hopping mobility is considered to be thermally activated, largely depending on the difference between the E_F and E_T. However, the $E_F - E_T$ offsets are comparable between the two doped polymers because of their similar Seebeck coefficients ($S = (E_F - E_T)/qT$). The large activation energy of the mobility cannot be explained by a small $E_F - E_T$ (~30 meV) in the doped N2200. A more reasonable explanation is that counterions serve as Coulomb traps, and therefore, the trapped charges require additional energy to hop to the E_T. These adverse effects appear to be minimized in the doped PDTzTI. Another benefit of the electrostatic strategy for increasing the doping level and electrical conductivity is the negligible effect on the Seebeck coefficient. This is evident as the doped PDTzTI shows a Seebeck coefficient similar to that of doped N2200 at the point of maximum conductivity. The present work offers a way to overcome the trade-off between electrical conductivity and Seebeck coefficient in optimizing the power factor.

In summary, we performed an in-depth study on vapor doping two n-type conjugated polymers (N2200 versus PDTzTI) for thermoelectrics. Doped N2200 film was characterized by an inefficient free-charge generation, poor charge transport, and a very low power factor of 0.06 $\mu W\ m^{-1}\ K^{-2}$. In contrast, doped PDTzTI demonstrated huge enhancements in terms of free-charge generation and transport, leading to a remarkable conductivity of 4.6 $S\ cm^{-1}$, power factor of 7.6 $\mu W\ m^{-1}\ K^{-2}$, and ZT of 0.01 at room temperature. Such large differences are rooted in their different molecular motifs. Particularly, the compact geometry of the building block DTzTI leads to PDTzTI with more planar and tightly packed backbone and minimized D−A character relative to N2200. These features endow PDTzTI with a better molecular ordering and charge delocalization, which help overcome the Coulomb interaction in the doped state. Consequently, free charges are more easily generated from charge−counterion pairs. It is worth mentioning that most experiences for designing thermoelectric polymers are transferred from those developed in OPV and OTFT fields where semiconducting properties are emphasized. However, the design of an ideal thermoelectric polymer should emphasize properties that affect the performance in the doped state. Our study provides useful insights into the factors governing the electrostatics in charged conjugated polymers and suggests a new direction for the design of better thermoelectric materials.

■ ASSOCIATED CONTENT

Supporting Information

The Supporting Information is available free of charge on the ACS Publications website at DOI: 10.1021/acsenergylett.9b00977.

Experimental section; DFT calculation; device fabrication and charaterization; in-plane thermal conductivity measurement (PDF)

■ AUTHOR INFORMATION

Corresponding Authors

*E-mail: jian.liu@rug.nl.
*E-mail: guoxg@sustech.edu.cn.
*E-mail: l.j.a.koster@rug.nl.

ORCID

Jian Liu: 0000-0002-6704-3895
Ryan C. Chiechi: 0000-0002-0895-2095
Derya Baran: 0000-0003-2196-8187
Giuseppe Portale: 0000-0002-4903-3159
Xugang Guo: 0000-0001-6193-637X
L. Jan Anton Koster: 0000-0002-6558-5295

Notes

The authors declare no competing financial interest.

■ ACKNOWLEDGMENTS

This work is supported by a grant from STW/NWO (VIDI 13476). This work is part of the research program of the Foundation of Fundamental Research on Matter (FOM), which is part of The Netherlands Organisation for Scientific Research (NWO). This is a publication by the FOM Focus Group "Next Generation Organic Photovoltaics", participating in the Dutch Institute for Fundamental Energy Research (DIFFER). X.G. is grateful to the NSFC (51573076), the Shenzhen Basic Research Fund (JCYJ20170817105905899), and the Shenzhen Peacock Plan Project (KQTD20140630110339343). D.B. acknowledges KAUST Competitive Research Grant (3737 GRG7) for financial support. J.L. thanks Shuyan Shao for inspiring discussions.

■ REFERENCES

(1) Lüssem, B.; Riede, M.; Leo, K. Doping of Organic Semiconductors. *Phys. Status Solidi A* **2013**, *210* (1), 9−43.
(2) Jacobs, I. E.; Moulé, A. J. Controlling Molecular Doping in Organic Semiconductors. *Adv. Mater.* **2017**, *29* (42), 1703063.
(3) Sun, Y.; Di, C.; Xu, W.; Zhu, D. Advances in N-Type Organic Thermoelectric Materials and Devices. *Adv. Electron. Mater.* **2019**, 1800825.
(4) Caliò, L.; Salado, M.; Kazim, S.; Ahmad, S. A Generic Route of Hydrophobic Doping in Hole Transporting Material to Increase Longevity of Perovskite Solar Cells. *Joule* **2018**, *2* (9), 1800−1815.
(5) Bubnova, O.; Khan, Z. U.; Malti, A.; Braun, S.; Fahlman, M.; Berggren, M.; Crispin, X. Optimization of the Thermoelectric Figure

DOI: 10.1021/acsenergylett.9b00977
ACS Energy Lett. 2019, 4, 1556−1564

of Merit in the Conducting Polymer Poly(3,4-Ethylenedioxythiophene). *Nat. Mater.* **2011**, *10* (6), 429−433.
(6) Huang, D.; Yao, H.; Cui, Y.; Zou, Y.; Zhang, F.; Wang, C.; Shen, H.; Jin, W.; Zhu, J.; Diao, Y.; et al. Conjugated-Backbone Effect of Organic Small Molecules for n-Type Thermoelectric Materials with ZT over 0.2. *J. Am. Chem. Soc.* **2017**, *139* (37), 13013−13023.
(7) Yuan, D.; Huang, D.; Rivero, S. M.; Carreras, A.; Zhang, C.; Zou, Y.; Jiao, X.; McNeill, C. R.; Zhu, X.; Di, C.; et al. Cholesteric Aggregation at the Quinoidal-to-Diradical Border Enabled Stable n-Doped Conductor. *Chem.* **2019**, *5*, 744.
(8) Kroon, R.; Kiefer, D.; Stegerer, D.; Yu, L.; Sommer, M.; Müller, C. Polar Side Chains Enhance Processability, Electrical Conductivity, and Thermal Stability of a Molecularly p-Doped Polythiophene. *Adv. Mater.* **2017**, *29*, 1700930.
(9) Wang, H.; Yu, C. Organic Thermoelectrics: Materials Preparation, Performance Optimization, and Device Integration. *Joule* **2019**, *3* (1), 53−80.
(10) Sun, L.; Liao, B.; Sheberla, D.; Kraemer, D.; Zhou, J.; Stach, E. A.; Zakharov, D.; Stavila, V.; Talin, A. A.; Ge, Y.; et al. A Microporous and Naturally Nanostructured Thermoelectric Metal-Organic Framework with Ultralow Thermal Conductivity. *Joule* **2017**, *1* (1), 168−177.
(11) Kiefer, D.; Kroon, R.; Hofmann, A. I.; Sun, H.; Liu, X.; Giovannitti, A.; Stegerer, D.; Cano, A.; Hynynen, J.; Yu, L.; et al. Double Doping of Conjugated Polymers with Monomer Molecular Dopants. *Nat. Mater.* **2019**, *18* (2), 149−155.
(12) Méndez, H.; Heimel, G.; Winkler, S.; Frisch, J.; Opitz, A.; Sauer, K.; Wegner, B.; Oehzelt, M.; Röthel, C.; Duhm, S.; et al. Charge-Transfer Crystallites as Molecular Electrical Dopants. *Nat. Commun.* **2015**, *6*, 8560.
(13) Salzmann, I.; Heimel, G.; Duhm, S.; Oehzelt, M.; Pingel, P.; George, B. M.; Schnegg, A.; Lips, K.; Blum, R.-P.; Vollmer, A.; et al. Intermolecular Hybridization Governs Molecular Electrical Doping. *Phys. Rev. Lett.* **2012**, *108* (3), 035502.
(14) Tietze, M. L.; Benduhn, J.; Pahner, P.; Nell, B.; Schwarze, M.; Kleemann, H.; Krammer, M.; Zojer, K.; Vandewal, K.; Leo, K. Elementary Steps in Electrical Doping of Organic Semiconductors. *Nat. Commun.* **2018**, *9* (1), 1182.
(15) Torabi, S.; Jahani, F.; Van Severen, I.; Kanimozhi, C.; Patil, S.; Havenith, R. W. A.; Chiechi, R. C.; Lutsen, L.; Vanderzande, D. J. M.; Cleij, T. J.; et al. Strategy for Enhancing the Dielectric Constant of Organic Semiconductors Without Sacrificing Charge Carrier Mobility and Solubility. *Adv. Funct. Mater.* **2015**, *25*, 150.
(16) Burke, J. H.; Bird, M. J. Energetics and Escape of Interchain-Delocalized Ion Pairs in Nonpolar Media. *Adv. Mater.* **2019**, *31*, 1806863.
(17) Arkhipov, V. I.; Emelianova, E. V.; Heremans, P.; Bässler, H. Analytic Model of Carrier Mobility in Doped Disordered Organic Semiconductors. *Phys. Rev. B: Condens. Matter Mater. Phys.* **2005**, *72* (23), 235202.
(18) Zuo, G.; Abdalla, H.; Kemerink, M. Impact of Doping on the Density of States and the Mobility in Organic Semiconductors. *Phys. Rev. B: Condens. Matter Mater. Phys.* **2016**, *93* (23), 235203.
(19) Yan, H.; Chen, Z.; Zheng, Y.; Newman, C.; Quinn, J. R.; Dötz, F.; Kastler, M.; Facchetti, A. A High-Mobility Electron-Transporting Polymer for Printed Transistors. *Nature* **2009**, *457* (7230), 679−686.
(20) Guo, X.; Watson, M. D. Conjugated Polymers from Naphthalene Bisimide. *Org. Lett.* **2008**, *10* (23), 5333−5336.
(21) Xu, Y.; Sun, H.; Li, W.; Lin, Y.-F.; Balestra, F.; Ghibaudo, G.; Noh, Y.-Y. Exploring the Charge Transport in Conjugated Polymers. *Adv. Mater.* **2017**, *29* (41), 1702729.
(22) Schlitz, R. a.; Brunetti, F. G.; Glaudell, A. M.; Miller, P. L.; Brady, M. a.; Takacs, C. J.; Hawker, C. J.; Chabinyc, M. L. Solubility-Limited Extrinsic n-Type Doping of a High Electron Mobility Polymer for Thermoelectric Applications. *Adv. Mater.* **2014**, *26* (18), 2825−2830.
(23) Shi, K.; Zhang, F.; Di, C.-A.; Yan, T.-W.; Zou, Y.; Zhou, X.; Zhu, D.; Wang, J.-Y.; Pei, J. Towards High Performance N-Type Thermoelectric Materials by Rational Modification of BDPPV Backbones. *J. Am. Chem. Soc.* **2015**, *137*, 6979.
(24) Liu, J.; Ye, G.; Zee, B. v. d.; Dong, J.; Qiu, X.; Liu, Y.; Portale, G.; Chiechi, R. C.; Koster, L. J. A. N-Type Organic Thermoelectrics of Donor-Acceptor Copolymers: Improved Power Factor by Molecular Tailoring of the Density of States. *Adv. Mater.* **2018**, *30*, 1804290.
(25) Wang, Y.; Nakano, M.; Michinobu, T.; Kiyota, Y.; Mori, T.; Takimiya, K. Naphthodithiophenediimide−Benzobisthiadiazole-Based Polymers: Versatile n-Type Materials for Field-Effect Transistors and Thermoelectric Devices. *Macromolecules* **2017**, *50* (3), 857−864.
(26) Yang, C.-Y.; Jin, W.-L.; Wang, J.; Ding, Y.-F.; Nong, S.; Shi, K.; Lu, Y.; Dai, Y.-Z.; Zhuang, F.-D.; Lei, T.; et al. Enhancing the N-Type Conductivity and Thermoelectric Performance of Donor-Acceptor Copolymers through Donor Engineering. *Adv. Mater.* **2018**, *30*, 1802850.
(27) Liu, J.; Qiu, L.; Alessandri, R.; Qiu, X.; Portale, G.; Dong, J.; Talsma, W.; Ye, G.; Sengrian, A. A.; Souza, P. C. T.; et al. Enhancing Molecular N-Type Doping of Donor-Acceptor Copolymers by Tailoring Side Chains. *Adv. Mater.* **2018**, *30* (7), 1704630.
(28) Kiefer, D.; Giovannitti, A.; Sun, H.; Biskup, T.; Hofmann, A.; Koopmans, M.; Cendra, C.; Weber, S.; Anton Koster, L. J.; Olsson, E.; et al. Enhanced N-Doping Efficiency of a Naphthalenediimide-Based Copolymer through Polar Side Chains for Organic Thermoelectrics. *ACS Energy Lett.* **2018**, *3* (2), 278−285.
(29) Niu, G.; Guo, X.; Wang, L. Review of Recent Progress in Chemical Stability of Perovskite Solar Cells. *J. Mater. Chem. A* **2015**, *3* (17), 8970−8980.
(30) Perry, E. E.; Chiu, C.-Y.; Moudgil, K.; Schlitz, R. A.; Takacs, C. J.; O'Hara, K. A.; Labram, J. G.; Glaudell, A. M.; Sherman, J. B.; Barlow, S.; et al. High Conductivity in a Nonplanar *n* -Doped Ambipolar Semiconducting Polymer. *Chem. Mater.* **2017**, *29*, 9742.
(31) Shin, Y.; Massetti, M.; Komber, H.; Biskup, T.; Nava, D.; Lanzani, G.; Caironi, M.; Sommer, M. Improving Miscibility of a Naphthalene Diimide-Bithiophene Copolymer with n-Type Dopants through the Incorporation of "Kinked" Monomers. *Adv. Electron. Mater.* **2018**, *4*, 1700581.
(32) Wang, S.; Sun, H.; Ail, U.; Vagin, M.; Persson, P. O. Å.; Andreasen, J. W.; Thiel, W.; Berggren, M.; Crispin, X.; Fazzi, D.; et al. Thermoelectric Properties of Solution-Processed n-Doped Ladder-Type Conducting Polymers. *Adv. Mater.* **2016**, *28* (48), 10764−10771.
(33) Wang, S.; Sun, H.; Erdmann, T.; Wang, G.; Fazzi, D.; Lappan, U.; Puttisong, Y.; Chen, Z.; Berggren, M.; Crispin, X.; et al. A Chemically Doped Naphthalenediimide-Bithiazole Polymer for n-Type Organic Thermoelectrics. *Adv. Mater.* **2018**, *30* (31), 1801898.
(34) Liu, J.; Maity, S.; Roosloot, N.; Qiu, X.; Qiu, L.; Chiechi, R. C.; Hummelen, J. C.; von Hauff, E.; Koster, L. J. A. The Effect of Electrostatic Interaction on N-Type Doping Efficiency of Fullerene Derivatives. *Adv. Electron. Mater.* **2019**, 1800959.
(35) Aubry, T. J.; Axtell, J. C.; Basile, V. M.; Winchell, K. J.; Lindemuth, J. R.; Porter, T. M.; Liu, J.-Y.; Alexandrova, A. N.; Kubiak, C. P.; Tolbert, S. H.; et al. Dodecaborane-Based Dopants Designed to Shield Anion Electrostatics Lead to Increased Carrier Mobility in a Doped Conjugated Polymer. *Adv. Mater.* **2019**, *31*, 1805647.
(36) Shi, Y.; Guo, H.; Qin, M.; Zhao, J.; Wang, Y.; Wang, H.; Wang, Y.; Facchetti, A.; Lu, X.; Guo, X. Thiazole Imide-Based All-Acceptor Homopolymer: Achieving High-Performance Unipolar Electron Transport in Organic Thin-Film Transistors. *Adv. Mater.* **2018**, *30* (10), 1705745.
(37) Guo, X.; Ortiz, R. P.; Zheng, Y.; Hu, Y.; Noh, Y.-Y.; Baeg, K.-J.; Facchetti, A.; Marks, T. J. Bithiophene-Imide-Based Polymeric Semiconductors for Field-Effect Transistors: Synthesis, Structure−Property Correlations, Charge Carrier Polarity, and Device Stability. *J. Am. Chem. Soc.* **2011**, *133* (5), 1405−1418.
(38) Guo, X.; Facchetti, A.; Marks, T. J. Imide- and Amide-Functionalized Polymer Semiconductors. *Chem. Rev.* **2014**, *114* (18), 8943−9021.

DOI: 10.1021/acsenergylett.9b00977
ACS Energy Lett. 2019, 4, 1556−1564

(39) Shi, Y.; Guo, H.; Qin, M.; Wang, Y.; Zhao, J.; Sun, H.; Wang, H.; Wang, Y.; Zhou, X.; Facchetti, A.; et al. Imide-Functionalized Thiazole-Based Polymer Semiconductors: Synthesis, Structure−Property Correlations, Charge Carrier Polarity, and Thin-Film Transistor Performance. *Chem. Mater.* **2018**, *30*, 7988.
(40) Estrada, L. A.; Liu, D. Y.; Salazar, D. H.; Dyer, A. L.; Reynolds, J. R. Poly[Bis-EDOT-Isoindigo]: An Electroactive Polymer Applied to Electrochemical Supercapacitors. *Macromolecules* **2012**, *45* (20), 8211−8220.
(41) Patel, S. N.; Glaudell, A. M.; Peterson, K. A.; Thomas, E. M.; O'Hara, K. A.; Lim, E.; Chabinyc, M. L. Morphology Controls the Thermoelectric Power Factor of a Doped Semiconducting Polymer. *Sci. Adv.* **2017**, *3*, e1700434.
(42) Qiu, L.; Liu, J.; Alessandri, R.; Qiu, X.; Koopmans, M.; Havenith, R. W. A.; Marrink, S. J.; Chiechi, R. C.; Anton Koster, L. J.; Hummelen, J. C. Enhancing Doping Efficiency by Improving Host-Dopant Miscibility for Fullerene-Based n-Type Thermoelectrics. *J. Mater. Chem. A* **2017**, *5* (40), 21234−21241.
(43) Kang, S. D.; Snyder, G. J. Charge-Transport Model for Conducting Polymers. *Nat. Mater.* **2017**, *16*, 252.
(44) Abdalla, H.; Zuo, G.; Kemerink, M. Range and Energetics of Charge Hopping in Organic Semiconductors. *Phys. Rev. B: Condens. Matter Mater. Phys.* **2017**, *96* (24), 241202.
(45) Kang, K.; Schott, S.; Venkateshvaran, D.; Broch, K.; Schweicher, G.; Harkin, D.; Jellett, C.; Nielsen, C. B.; McCulloch, I.; Sirringhaus, H. Investigation of the Thermoelectric Response in Conducting Polymers Doped by Solid-State Diffusion. *Mater. Today Phys.* **2019**, *8*, 112−122.
(46) Giovannitti, A.; Nielsen, C. B.; Sbircea, D.-T.; Inal, S.; Donahue, M.; Niazi, M. R.; Hanifi, D. A.; Amassian, A.; Malliaras, G. G.; Rivnay, J.; McCulloch, I. N-Type Organic Electrochemical Transistors with Stability in Water. *Nat. Commun.* **2016**, *7*, 13066.
(47) Naab, B. D.; Gu, X.; Kurosawa, T.; To, J. W. F.; Salleo, A.; Bao, Z. Role of Polymer Structure on the Conductivity of N-Doped Polymers. *Adv. Electron. Mater.* **2016**, *2* (5), 1600004.
(48) Pingel, P.; Schwarzl, R.; Neher, D. Effect of Molecular P-Doping on Hole Density and Mobility in Poly(3-Hexylthiophene). *Appl. Phys. Lett.* **2012**, *100* (14), 143303.
(49) Venkateshvaran, D.; Nikolka, M.; Sadhanala, A.; Lemaur, V.; Zelazny, M.; Kepa, M.; Hurhangee, M.; Kronemeijer, A. J.; Pecunia, V.; Nasrallah, I.; et al. Approaching Disorder-Free Transport in High-Mobility Conjugated Polymers. *Nature* **2014**, *515* (7527), 384−388.
(50) Etzold, F.; Howard, I. A.; Mauer, R.; Meister, M.; Kim, T.-D.; Lee, K.-S.; Baek, N. S.; Laquai, F. Ultrafast Exciton Dissociation Followed by Nongeminate Charge Recombination in PCDTBT:PCBM Photovoltaic Blends. *J. Am. Chem. Soc.* **2011**, *133* (24), 9469−9479.
(51) Baran, D.; Li, N.; Breton, A.-C.; Osvet, A.; Ameri, T.; Leclerc, M.; Brabec, C. J. Qualitative Analysis of Bulk-Heterojunction Solar Cells without Device Fabrication: An Elegant and Contactless Method. *J. Am. Chem. Soc.* **2014**, *136* (31), 10949−10955.
(52) Bakulin, A. A.; Rao, A.; Pavelyev, V. G.; van Loosdrecht, P. H. M.; Pshenichnikov, M. S.; Niedzialek, D.; Cornil, J.; Beljonne, D.; Friend, R. H. The Role of Driving Energy and Delocalized States for Charge Separation in Organic Semiconductors. *Science* **2012**, *335* (6074), 1340−1344.
(53) Steyrleuthner, R.; Schubert, M.; Howard, I.; Klaumünzer, B.; Schilling, K.; Chen, Z.; Saalfrank, P.; Laquai, F.; Facchetti, A.; Neher, D. Aggregation in a High-Mobility n-Type Low-Bandgap Copolymer with Implications on Semicrystalline Morphology. *J. Am. Chem. Soc.* **2012**, *134* (44), 18303−18317.
(54) Fazzi, D.; Caironi, M.; Castiglioni, C. Quantum-Chemical Insights into the Prediction of Charge Transport Parameters for a Naphthalenetetracarboxydiimide-Based Copolymer with Enhanced Electron Mobility. *J. Am. Chem. Soc.* **2011**, *133* (47), 19056−19059.
(55) Sirringhaus, H.; Brown, P. J.; Friend, R. H.; Nielsen, M. M.; Bechgaard, K.; Langeveld-Voss, B. M. W.; Spiering, A. J. H.; Janssen, R. A. J.; Meijer, E. W.; Herwig, P.; et al. Two-Dimensional Charge Transport in Self-Organized, High-Mobility Conjugated Polymers. *Nature* **1999**, *401* (6754), 685−688.
(56) Beljonne, D.; Cornil, J.; Sirringhaus, H.; Brown, P. J.; Shkunov, M.; Friend, R. H.; Brédas, J.-L. Optical Signature of Delocalized Polarons in Conjugated Polymers. *Adv. Funct. Mater.* **2001**, *11* (3), 229−234.

DOI: 10.1021/acsenergylett.9b00977
ACS Energy Lett. 2019, 4, 1556−1564